Roles of Phase Separation Mechanism and Coarsening in the Formation of Poly(methyl methacrylate) Asymmetric Membranes

Fu-Jya Tsai[†] and John M. Torkelson[*,†,‡]

Departments of Chemical Engineering and Materials Science and Engineering, Northwestern University, Evanston, Illinois 60208-3120. *Received May 30, 1989; Revised Manuscript Received July 25, 1989*

ABSTRACT: The effects of phase separation mechanism and flow properties on asymmetric poly(methyl methacrylate) (PMMA) membranes formed by thermally induced phase separation have been studied. Both cloud point and spinodal curves of a secondary standard PMMA (M_w = 93 300, M_n = 46 400) in sulfolane were determined by optical density methods and differential scanning calorimetry. In the absence of ripening/coalescence, an excellent agreement between the conditions of phase separation (in either the metastable or unstable region) and the membrane morphology observed by scanning electron microscopy is obtained. During the very early stage of phase separation by spinodal decomposition, a membrane with lacy structure results. In contrast, a structure composed of strings of small beads is a consequence of the early stage of nucleation and growth. The effect of ripening or coalescence has been demonstrated to be significant in determining the final membrane morphology for phase separation by both spinodal decomposition and nucleation and growth. A lacy structure can also be obtained for nucleation and growth due to the ripening or coalescence effect.

Introduction

The term asymmetric membrane refers to a skinned, dense film supported by a porous sublayer. The thin but dense film provides a barrier structure for rejecting certain, often undesired components while the porous sublayer provides a supporting structure with the purpose of offering a high flux for the passing components. Over the last several decades, synthetic polymer asymmetric membranes have been increasingly developed and applied to a variety of uses in the water treatment, food, medical, and other industries. Most of these polymer membranes were made from cellulosic materials and were prepared by the traditional phase inversion method.[1] Recently, the thermally induced phase separation technique has started to play an important role in the preparation of commercial, synthetic membranes from a variety of polymers. In contrast to the traditional phase-inversion method, the thermally induced phase separation technique is reported to be applicable for a wider variety of polymers and allows for better process control, for higher reproducibility, and for the production of higher void-volume product membranes.

The thermally induced phase separation method was first introduced by Castro[2,3] in the late 1970s and early 1980s. The basic idea behind this technique is to utilize heat as a latent solvent; in contrast, in the phase-inversion method, a non-solvent is added to the system. By lowering the temperature of an appropriate polymer–solvent system, phase separation can be induced, i.e., a transition from a one-phase homogeneous solution to a two-phase heterogeneous system. This technique has been applied to produce low density microcellular foams,[4–10] thermally reversible porous gels,[11–13] uniform porous membranes,[14–17] and asymmetric membranes.[18,19]

Recently, low density microcellular foams have been increasingly applied in preparing targets for inertial confinement fusion,[4–7] catalyst supports,[8] and controlled drug release systems.[9] Among these studies, Aubert and coworkers[9] indicated that by controlling the phase separation during quenching, the foam morphology, foam density, and cell size can be varied. In addition, changes in the foam morphology due to coarsening were reported by Aubert et al.[6] and Hikmer et al.[11] Polymers used in these studies include amorphous, semicrystalline or crystalline, and rigid-rod polymers.[10] Essentially, these foams can be prepared to possess uniform cell size. In 1985, Caneba and Soong[18] successfully produced asymmetric membranes from a poly(methyl methacrylate) (PMMA)/sulfolane system by applying this thermally induced phase separation technique. The basic idea behind their approach is first to confine a homogeneous polymer solution in a casting cell that is composed of a thermal-conductor sheet, a thermal-insulator plate, and a thermal-insulator template. This casting cell is then maintained at a temperature well above the cloud point of the polymer solution. By introducing a cooling medium that is in contact with the thermal-conductor sheet, phase separation is initiated and a temperature gradient within the polymer solution is then established. This results in different degrees of phase separation within the polymer solution along the direction of the temperature gradient. Thus, an anisotropic structure results. However, in their study, Caneba and Soong considered only spinodal decomposition as the mechanism of phase separation.

At the present time, a full understanding of the precise mechanism of the membrane formation and the effect of the liquid–liquid phase separation on the resulting membrane microstructure is lacking. Furthermore, except for one preliminary study,[20] little attention has been paid to the role of coarsening during the later stages of phase separation on the resulting membrane microstructure. We should note that Caneba and Soong's approach[18] for preparing asymmetric membranes has inspired our work. On the basis of the phase diagram determined that includes both cloud point and spinodal curves, this present study provides more detailed information on membrane formation by also considering the possibility of nucleation and growth in this thermally induced phase separation technique. This study emphasizes understanding the role of phase separation mechanism on the formation of asym-

* To whom correspondence should be addressed.
† Department of Chemical Engineering.
‡ Department of Materials Science and Engineering.

0024-9297/90/2223-0775$02.50/0

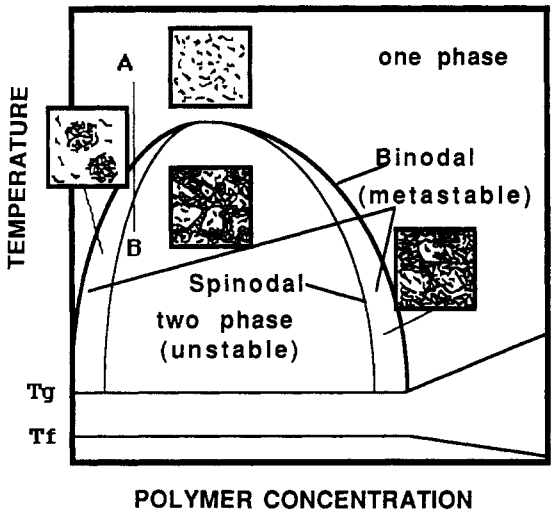

Figure 1. Schematic upper critical temperature solution phase diagram illustrating the expected variation in morphology of a polymer/solvent solution system: T_g, the glass transition temperature of the polymer solution; T_f, the solidification point of the solvent.

metric membranes through the use of the thermally induced phase separation method and illustrates the importance of the effects of ripening or coalescence in liquid–liquid phase separation of polymer solutions. In addition, the effects of original composition, quenching rate, and quenching depth are discussed. It should be noted that this understanding should also be applicable in guiding development of microcellular foams, thermally reversible porous gels, and other porous membranes, which can be prepared by similar processes.

Liquid–Liquid Phase Separation

Smolders et al.[21,22] pointed out that structure formation in polymer membranes can be classified into three mechanisms: (1) liquid–liquid phase separation; (2) gelation; and (3) crystallization. Gelation involves the formation of the microcrystalline regions perhaps not larger than the nucleus and generally takes place at high polymer concentrations. Gelation has also been reported by Arnauts and Berghmans[23] to be associated with cooling a noncrystalline atactic polystyrene/decalin system. They suggested that the gelation of this noncrystallizable system is due to a liquid–liquid phase separation arrested by a vitrification process. A solution of atactic polystyrene in cyclohexanol was also reported to form thermoreversible, microporous gels.[11] In our study, we will focus on asymmetric membranes made from noncrystalline systems. Therefore, only liquid–liquid phase separation processes as well as possible gelation due to the vitrification process will be considered for our membrane formation.

A typical temperature-composition phase diagram exhibiting an upper critical solution temperature (UCST) for a polymer solution is shown in Figure 1. The heavy solid curve shown in Figure 1 is referred to as the binodal curve; this separates the stable one-phase region from the region in which two phases coexist at equilibrium. By definition, the binodal is the locus of points for which the chemical potentials of each component are equal in both phases. The light solid curve shown in Figure 1 is referred to as the spinodal curve, which demarcates the two-phase region into metastable and unstable portions. By definition, the spinodal curve is the locus of points for which the second derivative of the Gibbs free energy of mixing equals zero. When a sample of known composition is taken from the one-phase region to the two-phase region, the sample may undergo phase separation by one of two distinct mechanisms depending on the quenching temperature.

In the metastable region, the sample is believed to undergo phase separation by a nucleation and growth mechanism. The nucleation of the secondary phase has an energy barrier due to the surface energy of the nucleus–matrix interface. After a nucleus reaches a critical size, it becomes stable and grows by the diffusion of molecules to the secondary phase. Just outside of the precipitate, the matrix is depleted, and diffusion is by the normal mechanism in which the coefficient of diffusion is positive. Alternatively, when the system is in the unstable region, phase separation is carried out by a process known as spinodal decomposition. The main feature of spinodal decomposition is an uphill diffusion; i.e., the diffusion coefficient is negative. This is best understood by the Cahn–Hilliard treatment.[24,25] Schematic illustrations of the resulting morphology by both nucleation and growth and spinodal decomposition mechanisms are shown in Figure 1. During nucleation and growth, the nuclei grow in extent without changing composition. However, during the early stages of spinodal decomposition, it is believed that the composition departing from the average changes exponentially with time whereas the volume fractions of the phases remain constant. A characteristic interconnected phase morphology is its main feature.

By varying the composition and temperature, polymer solutions can be brought into different regions for study. However, from the kinetic point of view, the cooling rate and quenching period are two important parameters to be considered. For example, if one follows a quenching route from point A to point B shown in Figure 1, the cooling rate will be the dominant factor in determining the phase separation mechanism. If the cooling rate is fairly fast, phase separation will be dominated by spinodal decomposition. In contrast, if the cooling rate is slow enough for the formation of nuclei, phase separation may be dominated by nucleation and growth. In addition, the effect of ripening or coalescence has been reported for a variety of systems and has been shown to be of vital importance in determining the final morphology during the later stages of phase separation.[21,26,27]

In order to freeze the resulting membrane structure at a desired point in time, the phase separated system has to be quenched quickly into regions in which temperature is below either the glass transition temperature (T_g) of the polymer solution or the solidification point (T_f) of the solvent. In order to remove solvent while not perturbing the resulting polymer microstructure, either solvent extraction or freeze-drying can be used.

Experimental Section

Secondary standard PMMA (M_w = 93 300, M_n = 46 400) was purchased from Scientific Polymer Products, Inc. Reagent grade sulfolane (tetramethylene sulfone) was obtained from Aldrich. All materials were used without any further purification.

The cloud point of the phase diagram was determined by the optical density method with an IBM 9410 UV/visible spectrophotometer. The measurements were made by loading the sample in a water-jacketed cell at a temperature some 15 °C above the expected cloud point. This sample cell then was subsequently cooled until a sharp increase in optical density was observed. An optical wavelength of 800 nm was used for monitoring. The spinodal curve of the phase diagram, glass transition temperature (T_g), and solidification point of the solvent were determined by thermal analysis with a Perkin-Elmer DSC-2 differential scanning calorimeter.

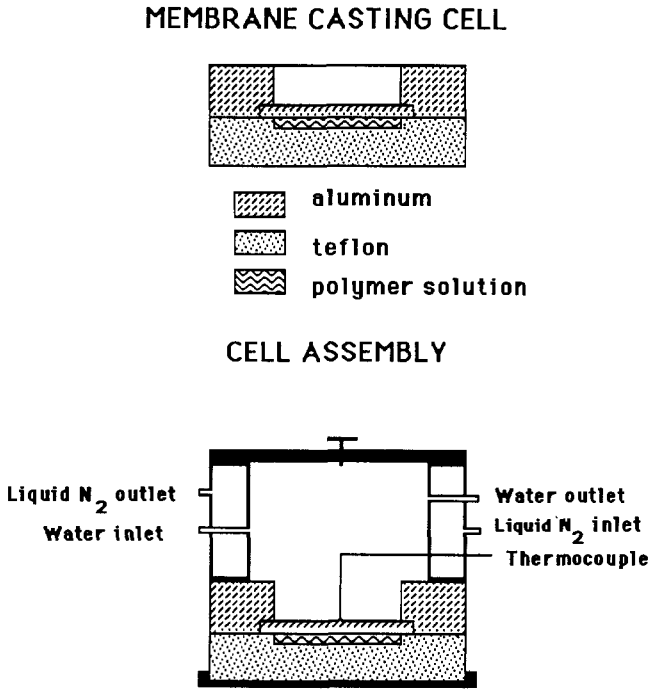

Figure 2. Schematic diagrams of the membrane casting cell and the membrane casting cell assembly used for controlling the temperature of the cell.

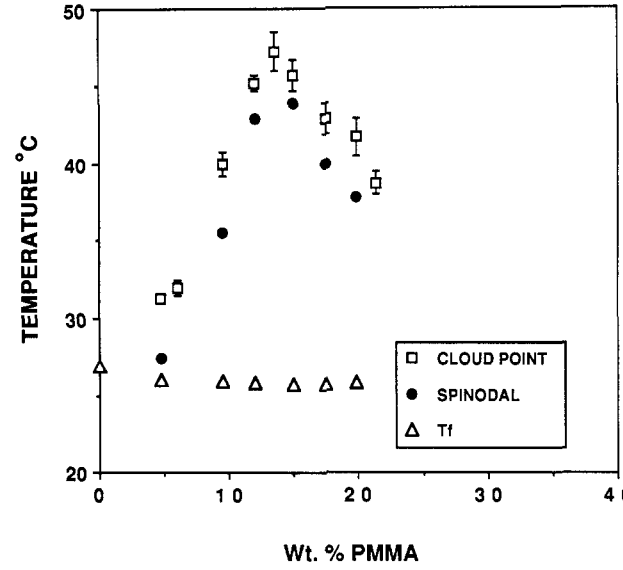

Figure 3. Phase diagram for a secondary standard PMMA (M_w = 93 300, M_n = 46 400)/sulfolane system. The cloud point curve is determined by the optical density method. The spinodal curve and T_f are determined by differential scanning calorimetry. T_f represents the solidification point of the solvent-rich phase under equilibrium condition.

The thermal-inversion method[18] was used to prepare the asymmetric membranes. The initial homogeneous polymer solution was confined within a thin aluminum sheet and a Teflon block. A 5-in. diameter compartment for holding the original polymer solution was inserted in an integrated manner on top of the Teflon block. The Teflon compartment is 500 μm in thickness. The casting cell was then held inside the cell assembly. The detailed design of this setup is shown schematically in Figure 2. Temperature control was achieved by circulating constant temperature water through the cell assembly. For freezing the membrane structure, liquid nitrogen can be introduced either into the annular space at the side of assembly or directly onto the top of the casting cell. The temperature of polymer solution in contact with the metal sheet was monitored by placing a chromel–alumel thermocouple inside the cell assembly.

After the membrane was frozen, distilled water was used for extracting the solvent, sulfolane. In order to preserve the microstructure as far as possible, the water and some remaining solvent were removed by freeze-drying at −55 °C with a VirTis Bench Top freeze-dryer. The desired pressure for this freeze-drying is less than 1 mTorr. The resulting membranes were coated by gold sputtering for further study by scanning electron microscopy (SEM) with a Hitachi S-570 SEM. Cross sections of the resulting membranes were prepared by freeze-fracturing under liquid nitrogen.

Results and Discussion

Phase Diagram Determination. A wide range scan from 200 to 900 nm was carried out on PMMA/sulfolane solutions by UV/visible absorbance spectroscopy. No evidence of any absorption from either PMMA or sulfolane was found at 800-nm wavelength. Thus, as the cloud point temperature is approached from above, the sharp increase in optical density of the solutions can be explained by the scattering of incident light upon formation of large aggregates due to phase separation. (A complete description of the use and illustration of the sensitivity of optical density methods in determining cloud point curves of liquid polymer systems is given in a previous study[28] by Tsai and Torkelson.) The cloud point curve shown in Figure 3 is determined by this approach for the secondary standard PMMA/sulfolane system. In Caneba and Soong's study,[18,29] only one polymer solution sample was used to determine the entire cloud point curve with a pulsed FT-NMR technique and their theoretical calculation. The optical density method used in determining the cloud point curve shown in Figure 3 is more direct and offers greater accuracy in investigating further the effect of phase separation on the resulting membrane structure.

In comparison with the result obtained by Caneba and Soong[29] for a monodisperse PMMA (M_w = 54 000, $M_w/M_n < 1.07$)/sulfolane system, the entire cloud point curve of our secondary standard PMMA/sulfolane system shifts toward higher PMMA composition in a temperature–composition coordination. This rather peculiar shift of the cloud point curve for the secondary standard PMMA/sulfolane system was consistent with our results in a previous study[20] for the PMMA/xylene system and was also reported by Caneba and Soong for a polydisperse PMMA (M_w > 100 000)/sulfolane system. This phenomenon has been well explained in a previous study by Scott[30] in terms of the polydispersity of the system. Scott determined that in a polydisperse polymer system the low molecular weight material makes the higher molecular weight fractions more soluble.

In contrast to a monodisperse polymer/solvent system, a cloud point curve does not coincide with the binodal curve for a polydisperse polymer/solvent system.[31] We should note that this secondary standard PMMA (M_w/M_n = 2.0) is not a monodisperse polymer. Therefore, no attempt is being made to use the tie lines of the cloud point curve given in Figure 3 for quantitative analysis of equilibrium concentrations in each phase. However, we believe that the cloud point curve determined through the optical density method for this system can offer a good basis for the SEM study in terms of dividing the homogeneous and heterogeneous regions.

The spinodal curve is determined by thermal analysis with a DSC. When a homogeneous solution is cooled in the DSC at a rate high enough to prevent phase separation by nucleation and growth, an exotherm is observed

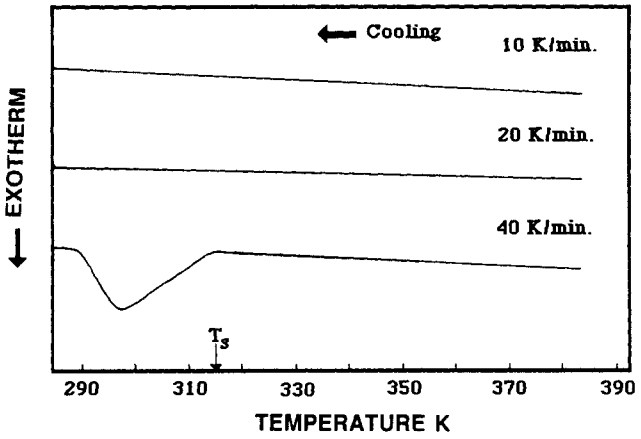

Figure 4. Spinodal temperature and cooling rate effects determined by differential scanning calorimetry for a 12 wt % PMMA solution.

at a certain temperature range. This technique was first used in a previous study by Smolders et al.[32] for a poly(phenylene oxide) (PPO)/toluene system. When the solution is reheated, Smolders et al. observed a very broad endotherm that became larger with increasing annealing time. The endotherm ending at a higher temperature is referred to as the cloud point temperature.[32]

Figure 4 illustrates a typical example for our determination of the spinodal curve. A 12 wt % PMMA/88 wt % sulfolane solution is cooled at three different rates from 100 to 0 °C. At low cooling rates, 10 and 20 °C/min, there is no thermal transition observed. In contrast, at the rate of 40 °C/min, an exotherm is evident. This result indicates the appearance of the exotherm (resulting from the spinodal decomposition) is dependent upon the cooling rate. Fast quenching increases the possibility of avoiding any phase separation by nucleation and growth and enhances the likelihood that virtually all phase separation is due to spinodal decomposition. However, the necessary quenching rate to avoid nucleation and growth varies with the system studied. With a more mobile system, a higher quenching rate is needed to observe the exotherm. In van Emmerik and Smolders's study,[32] they were able to observe the exotherm for the PPO/toluene system by using the cooling rate of 16 °C/min. However, in the current PMMA–sulfolane system, we are not able to observe the exotherm until the cooling rate increases to 40 °C/min. Furthermore, in contrast to the results by van Emmerik and Smolders,[32] we do not see a broad endotherm upon direct reheating of the solution; we believe this is due to the fact that upon heating the system goes back gradually to its homogeneous state. The absence of the endotherm upon heating is presumably due to the fact that the broad molecular weight distribution of the secondary standard PMMA reduces the sensitivity to detect the cloud point for this system and/or the phase separation time is not long enough for detecting this change. Nevertheless, this technique can be a very convenient way to determine the spinodal temperatures if the system is sufficiently viscous.

Thermal Analysis. In order to gain insight into the role gelation plays in determining the final membrane morphology, thermal analysis by DSC was done over the entire polymer concentration region under the demixing curve. Thermal analysis was carried out by quenching the samples from the temperature well above the demixing curve to −15 °C at a rate of 160 °C/min. Upon heating the quenched samples at a rate of 5 °C/min, the thermograms were then recorded. Figure 5 shows several typical thermograms for this measurement. For a pure sulfolane solvent, only one endothermic peak due to melting of the solvent is observed. (This melting temperature measured by DSC is consistent with the melting temperature of sulfolane given in the literature.[33]) In contrast, two endothermic peaks are observed for the samples of PMMA/sulfolane solution with various composition ratios.

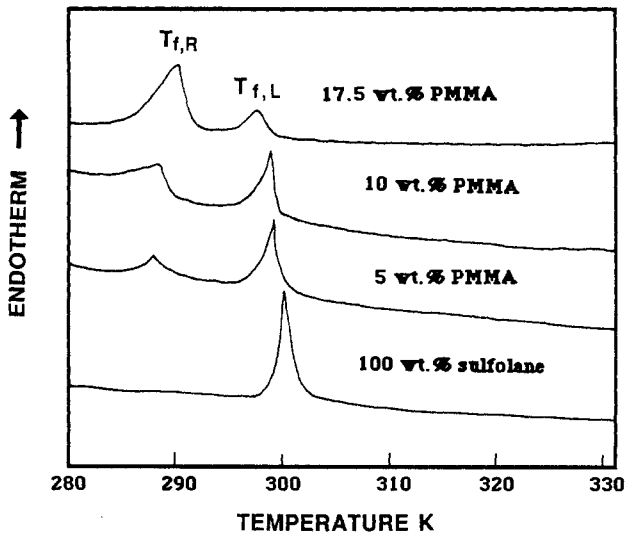

Figure 5. Examples of thermograms used to determine the freezing point ($T_{f,R}$) of the polymer-rich phase domain and the freezing point ($T_{f,L}$) of the polymer-lean phase domain. Quenching rate used in this experiment is 160 °C/min.

It is believed that both the DSC endotherms might result from solvent melting in each phase, depressed by differing amounts of dissolved polymer. The endothermic peak ($T_{f,R}$) at the lower temperatures is associated with the polymer-rich phase, whereas the other ($T_{f,L}$) is associated with the polymer-lean phase. In addition, Figure 5 shows a decreasing trend in the sizes of higher temperature endotherms ($T_{f,L}$) but an increasing trend in the sizes of lower temperature endotherms ($T_{f,R}$), with increasing overall PMMA concentration. This result is consistent with the fact that the total volume of polymer-lean phase decreases but the total volume of polymer-rich phase increases, with increasing overall polymer composition. Furthermore, a slight drift, but in an opposite manner, in the temperature of each peak is observed with increasing overall polymer composition. This result is presumably due to the fact that composition equilibration has not been reached in this time frame. In contrast, by using a cooling rate of 40 °C/min for the thermal analysis, the temperature of each peak remains roughly invariant with increasing overall polymer concentration. It is believed that during the quenching the lower cooling rate allows composition equilibration to be more nearly achieved. The freezing temperatures of the solvent-rich phase measured as a function of overall polymer concentration are given in Figure 3. Within experimental error, freezing temperatures given in Figure 3 are concentration-independent and represent essentially equilibrium values.

Ripening/Coalescence Effect. Figure 6 shows scanning electron micrographs of the thermal-casting membranes prepared from a starting solution which was 10 wt % secondary standard PMMA/90 wt % sulfolane. These scanning electron micrographs are views of the surface in contact with the thermal-insulator block. (The

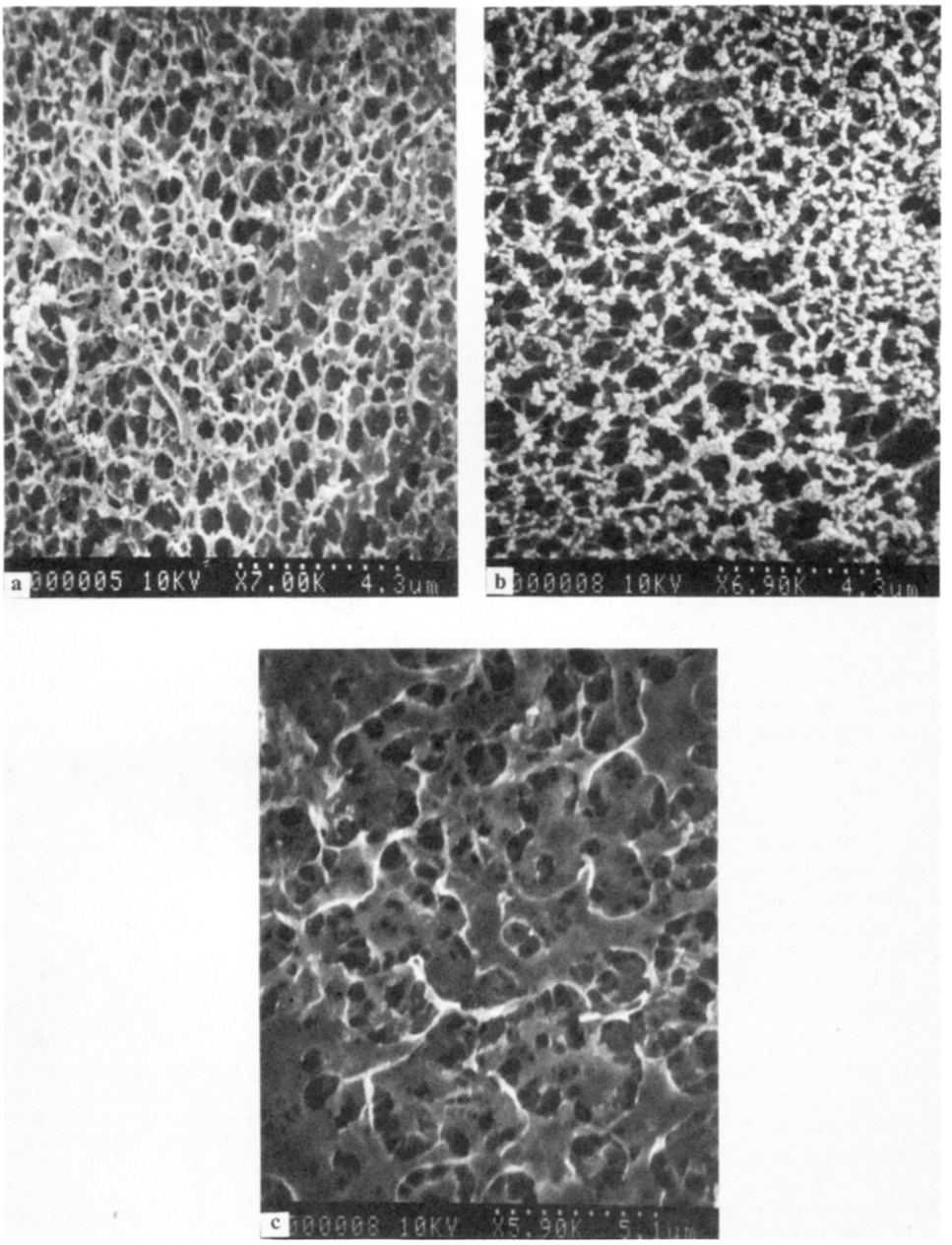

Figure 6. Scanning electron micrograph of the surface of the PMMA membrane in contact with the thermal-insulator plate. (a) Membrane prepared by quenching a 10 wt % PMMA solution directly into liquid nitrogen. (b) Membrane prepared by quenching a 10 wt % PMMA solution to 27 °C and holding for 5 min. (c) Membrane prepared by quenching a 10 wt % PMMA solution to 27 °C and holding for 30 min.

views of the surface in contact with the thin thermal-conductor sheet for membranes studied are discussed later in the asymmetry section of this paper.) Figure 6a shows the resulting microstructure for the membrane produced by quenching the solution directly into liquid nitrogen prior to freeze-drying. This quenching step lasted on the order of a second. This fast quenching procedure assures the investigation of the very early stages of phase separation by spinodal decomposition owing to the fact that spinodal decomposition can take place instantaneously while nucleation and growth takes a longer time to initiate. (A previous study by Tsai and Torkelson[28] on a similarly very viscous system, oligomeric polystyrene/polybutadiene, confirmed the fact that spinodal decomposition takes place instantaneously.) The membrane in Figure 6a exhibits a lacy structure with pore size on the order of 0.45 μm. In accordance with the phase diagram in Figure 3, it is believed that this interconnected structure is a consequence of the very early stage of phase separation dominated by a spinodal decomposition process.

In order to study the ripening/coalescence effect, a starting solution with the same composition as above was quenched to 27 °C and held for either 5 or 30 min prior to freezing and freeze-drying. Figure 6b shows the resulting microstructure for the membrane produced by quenching the solution to 27 °C and holding for 5 min. The lacy structure exhibits a pore size similar to that in Figure 6a; this indicates that the ripening/coalescence effect has not come into play or has played merely an insignificant role at this stage of phase separation. In addition, the lacy structure suggests that spinodal decomposition still dominates the phase separation process at this temperature region. However, beadlike clusters dispersed on the top of the lacy structure were observed. This beadlike cluster structure is presumably formed by an agglomeration of the polymer-lean phase during the freeze-drying process.

Figure 6c shows the resulting microstructure for the membrane produced by quenching the solution to 27 °C and holding for 30 min. This significantly different microstructure is strong evidence for ripening or coalescence of the polymer-rich phase during the later stage of phase separation by spinodal decomposition. McMaster[34] studied liquid–liquid phase transition phenomena in a polymer blend system. He found that for an interconnected structure, the mechanism of coarsening is viscous flow driven by interfacial tension (coalescence), whereas the dispersed structure coarsens by Ostwald ripening. A comparison of Figure 6b with Figure 6c clearly illustrates that the coarseness of the interconnected phase domains increases from 5 to 30 min of aging. According to McMaster's finding, this result suggests that flow properties of this polymer system play a vital role during the later stages of phase separation by spinodal decomposition.

This effect of coarsening was also found in a PMMA/xylene system studied previously.[20] Coarsening of the PMMA/sulfolane system proceeds much more slowly than that of the PMMA/xylene system due to the fact that the sulfolane system has higher viscosity than the xylene system. By comparison with the previous study, it is clear that the coarsening of the interconnected, two-phase PMMA/xylene system (25 wt % PMMA quenched to 18 °C for 20 min prior to freeze-drying) is more significant than that of the interconnected, two-phase PMMA/sulfolane system (10 wt % PMMA quenched to 27 °C for 30 min prior to freeze-drying). This result is consistent with McMaster's finding and is associated with the much lower viscosity of the PMMA/xylene system. We should note that in the current study, no attempt is being made to distinguish quantitatively between the two different mechanisms, coalescence and Ostward ripening, for the coarsening in the later stages of phase separation. Future study will involve quantitative analysis of this coarsening by comparison with several theoretical treatments.[27]

Effect of Phase Separation Mechanism. In order to study the effect of phase separation mechanism in the absence of ripening/coalescence effects on the resulting membrane morphology, two strategies were used. One is to study the very early stage of phase separation structure by quickly quenching samples either into the metastable region for nucleation and growth or into the unstable region for spinodal decomposition. On the basis of the phase diagram obtained, 5 wt % PMMA at 30 °C is most likely in the metastable region and will result in phase separation by nucleation and growth. In contrast, 13.5 wt % PMMA at 30 °C was chosen to investigate spinodal decomposition as this starting solution composition is most likely close to the critical composition of the binary phase diagram. Membranes made from both 5 wt % and 13.5 wt % PMMA samples were quickly quenched to 30 °C and stored for only about 1 min prior to freeze-drying.

Figure 7 shows the cross-section view of the resulting microstructure for the membrane produced by quenching a 5 wt % PMMA solution to 30 °C and holding for about 1 min. The structure is seen to consist of strings of small beads and some nodular structures (~1–2 μm) agglomerated by small beads rather than an interconnected structure. In addition, the resulting membrane is very fragile, which agrees well with prior observations[6] of a mechanically weak powder being formed by a presumed nucleation and growth mechanism. This resulting structure is consistent with what was expected except that the small beads are knitting together. This

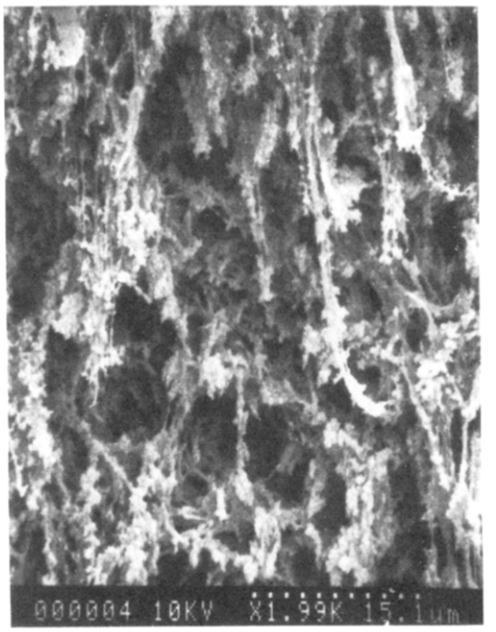

Figure 7. Scanning electron micrograph of the cross section of the middle portion of a PMMA membrane. The membrane was prepared by quenching a 5 wt % PMMA solution to 30 °C and holding for about 1 min.

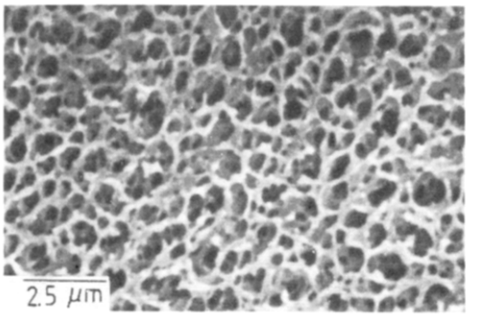

Figure 8. Scanning electron micrograph of the surface of the PMMA membrane in contact with the thermal-insulator plate. The membrane was prepared by quenching a 13.5 wt % PMMA solution to 30 °C and holding for about 1 min.

is believed to be a consequence of the coalescence of the polymer-rich phase droplets (nuclei) that were produced by the nucleation and growth mechanism upon phase separation.

Figure 8 shows the surface view of the resulting microstructure for the membrane produced by quenching a 13.5 wt % PMMA solution to 30 °C and holding for about 1 min. In contrast, an interconnected and lacy structure with pore size on the oroer of 0.5 μm was seen. In addition, this membrane has a much higher material strength than that of the membrane shown in Figure 7. This resulting interconnected structure and the stronger material strength obtained are consistent with what is expected for spinodal decomposition.

The second method for studying the effect of phase separation mechanism is to vary the cooling rate for a given cooling route that passes through both metastable and unstable regions. By slowly cooling a starting solution whose composition is not close to the critical concentration, nucleation and growth should dominate the phase separation process. In contrast, by quickly quenching, spinodal decomposition should be prevalent. In this cooling rate study, a 10 wt % PMMA sample was chosen as it allows access to both metastable and unstable regions. Membranes made from a 10 wt % PMMA sam-

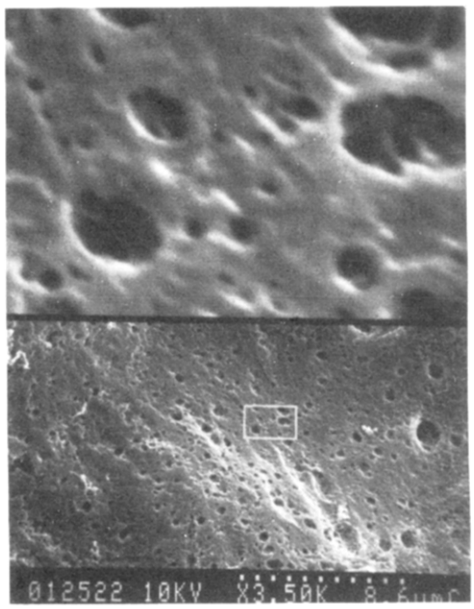

Figure 9. Scanning electron micrograph of the surface of the PMMA membrane in contact with the thermal-insulator plate. The membrane was prepared by slowly cooling to a 10 wt % PMMA solution to 27 °C and holding for 5 min. (The scale bar representing 8.6 μm for the lower micrograph represents 0.86 μm for the upper micrograph.)

ple were either quickly quenched or slowly cooled to 27 °C and held for another 5 min prior to freeze-drying.

Figure 9 shows the surface view of the resulting microstructure for the membrane produced by slowly cooling a 10 wt % PMMA solution to 27 °C prior to freezing to liquid-nitrogen temperature. In contrast to the result obtained by quickly quenching the same composition solution to 27 °C prior to freezing to liquid-nitrogen temperature (see Figure 6b), a structure in which circular pores dispersed randomly in the polymer matrix results. At higher magnification, a structure with cells connected by small pores is observed. A similar structure has been found in a crystallizable system[17] and was attributed to be a consequence of phase separation through nucleation and growth. In addition, the membrane produced by slow cooling is much more fragile than the membrane produced by fast quenching. A similar result was also observed by Aubert and Clough[6] for a polystyrene solution system. Aubert and Clough[6] reported that with slow quenching rates, only powder and not a foam was produced for their system. Thus, it is believed that the nucleation and growth dominates the phase separation for this 10 wt % PMMA sample obtained by slow cooling.[35]

Composition and Quenching Depth Effects. Variations of the resulting membrane structure produced in different regions under the cloud point curve were studied by changing the composition and quench depth. In addition, the effect of quenching period was also investigated. Compositions below (5 wt % PMMA) and above (17.5 wt % PMMA) the likely critical composition were chosen for this study.

Membranes made from the 5 wt % PMMA/95 wt % sulfolane solution were prepared by suddenly quenching from its homogeneous state to three different conditions: (1) 28 °C for 5 min followed by freezing to liquid-nitrogen temperature, (2) 28 °C for 30 min followed by freezing to liquid-nitrogen temperature, and (3) liquid-nitrogen temperature directly.

Figure 10 shows two surface views of the resulting microstructure under differing magnifications for the membrane produced by quenching the 5 wt % PMMA solution to 28 °C and holding for 5 min prior to freezing to liquid-nitrogen temperature. Figure 10a shows a weakly "lacy" structure. According to the traditional criterion,[14,17] the "lacy" structure can be considered to be a consequence of phase separation by spinodal decomposition. However, Figure 10a was taken under low magnification (×990). After further comparison with a micrograph (Figure 10b) taken at higher magnification (×15 000), it appears that the "lacy" structure is actually composed of strings of small beadlike particles. This is presumably due to an agglomeration of polymer-rich phase droplets formed during the later stage of phase separation by nucleation and growth.

Figure 11 shows the surface view of the membrane prepared by quenching the same composition solution to 28 °C but storing for a longer time period (30 min). The interconnected, lacy structure shown in Figure 11 suggests that the structure results from a strong ripening/coalescence effect. However, this result suggests that, in the presence of the ripening/coalescence effect, the "lacy" structure is not necessarily a consequence of phase separation by spinodal decomposition.

Figure 12 shows the surface view of the resulting microstructure for the membrane produced by suddenly quenching a 5 wt % PMMA solution to liquid-nitrogen temperature. In contrast to Figures 10 and 11, Figure 12 shows a sound interconnected, lacy structure with the pore size on the order of 0.1 μm. A comparison of Figure 12 with Figure 10 (under the same magnification) strongly suggests that this interconnected structure is a consequence of phase separation by spinodal decomposition. According to the phase diagram in Figure 3, it is believed that the spinodal decomposition process for the 5 wt % PMMA solution must take place instantaneously before the sample reaches T_f.

Membranes made from 17.5 wt % PMMA/82.5 wt % sulfolane were prepared in the following two different ways: (1) quenching to liquid-nitrogen temperature and (2) quenching to 34 °C for 5 min followed by freezing to liquid-nitrogen temperature.

Figure 13a shows the surface view of the resulting microstructure for the membrane produced by suddenly quenching the 17.5 wt % PMMA solution to liquid-nitrogen temperature. The structure is composed of bicontinuous phases (voids in micrograph indicate spaces that were originally occupied by the sulfolane solvent). Under the condition of fast quenching, it is believed that the interconnected structure is due to the phase separation by spinodal decomposition.

Figure 13b shows the surface view of the resulting microstructure of the membrane in the case of quenching to 34 °C for 5 min prior to freezing to liquid-nitrogen temperature. The surface is in contact with the thermal-insulator block. A view of the corresponding opposite surface in contact with the thin aluminum plate is shown in the section of the paper describing asymmetry. Figure 13b shows a lacy structure with pore size on the order of 0.3 μm. By comparison with the results obtained in the mechanism effect study, this structure can be attributed to a spinodal decomposition process. This is confirmed by checking the cloud point and spinodal temperatures for this sample based on the phase diagram in Figure 3. Most importantly, in the absence of coalescence or ripening effects, this microscopic observation of the phase-separated structure through a quick freezing and freeze-drying process may offer an opportunity to determine the spinodal curve or to confirm the spinodal curve determined by other techniques. However, for a

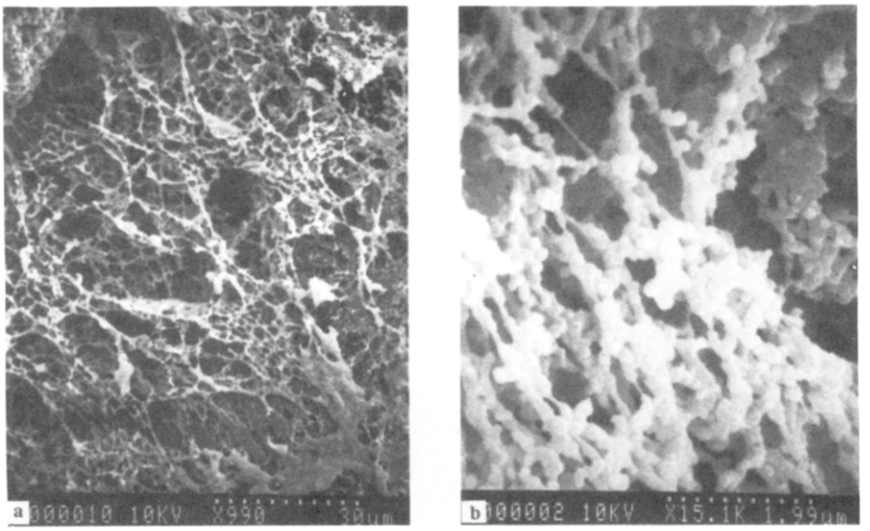

Figure 10. Scanning electron micrographs of the surface of the PMMA membrane in contact with the thermal-insulator plate under different magnifications: (a) ×990 with scale bar representing 30 μm; (b) ×15 000 with scale bar representing 1.99 μm. The membrane was prepared by quenching a 5 wt % PMMA solution to 28 °C and holding for 5 min.

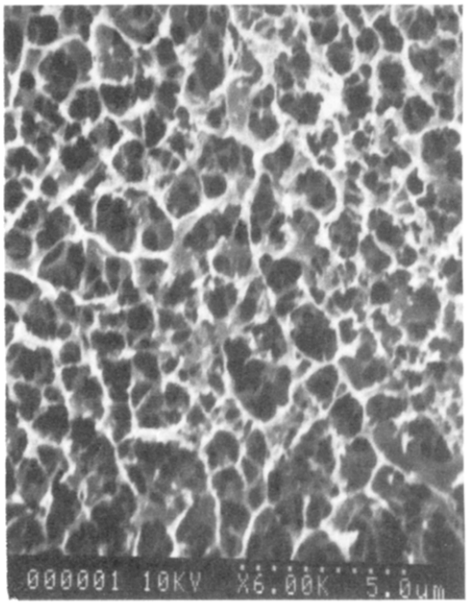

Figure 11. Scanning electron micrograph of the surface of the PMMA membrane in contact with the thermal-insulator plate. The membrane was prepared by quenching a 5 wt % PMMA solution to 28 °C and holding for 30 min.

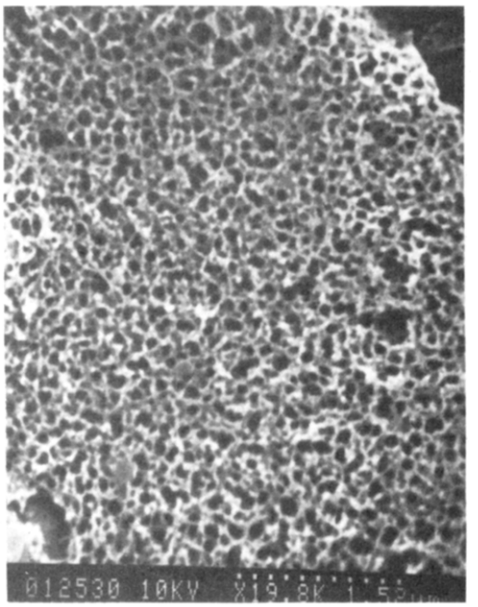

Figure 12. Scanning electron micrograph of the surface of the PMMA membrane in contact with the thermal-insulator plate. The membrane was prepared by quenching a 5 wt % PMMA solution directly into liquid nitrogen.

dilute or nonviscous polymer solution, the flow properties of the system may become more important in determining the final morphology. Some difficulties may be expected in using this method. Further study will focus on a highly mobile system such as PMMA in *tert*-butyl alcohol.

Asymmetry. In this asymmetry study, surfaces in contact with both the thin aluminum sheet and Teflon block were examined by SEM for all the membranes prepared. In addition, cross-section views for some membranes were also investigated. In contrast to the previous results by Caneba and Soong,[18] all the membranes prepared in our study show a characteristic of anisotropy.

Figure 14 shows the views of the surface in contact with the thin aluminum sheet for the membranes prepared from (a) the 10 wt % PMMA sample and (b) the 17.5 wt % PMMA sample. Figure 14a corresponds to the opposite surface view of the same membrane shown in Figure 6a. Comparison of the results in Figures 14a and 6a illustrates the feature of asymmetry. For a membrane prepared from the 10 wt % PMMA/90 wt % sulfolane solution, the surface (Figure 6a) in contact with the Teflon block (thermal-insulator plate) shows that the average pore size of this surface is on the order of 0.45 μm while the surface (Figure 14a) in contact with the thin aluminum sheets exhibits a dense structure. Figure 14b corresponds to the opposite surface view of the same membrane shown in Figure 13a. Similarly, comparison of the results in Figures 14b and 13a for the membrane prepared from a 17.5 wt % PMMA solution illustrates evident asymmetry. The surface (Figure 13a) in contact with the thermal-insulator plate exhibits an average pore size on the order of 0.5 μm while the surface (Figure 14b) in contact with the thin aluminum sheet exhibits an average pore size smaller than 0.1 μm.

Figure 15 exhibits the cross-section view of the membrane prepared by quenching a 5 wt % PMMA solution to 27 °C for 5 min prior to freezing. Figure 15 shows a characteristic of fingerlike asymmetry. The surface in contact with the thin aluminum sheet exhibits a thin but

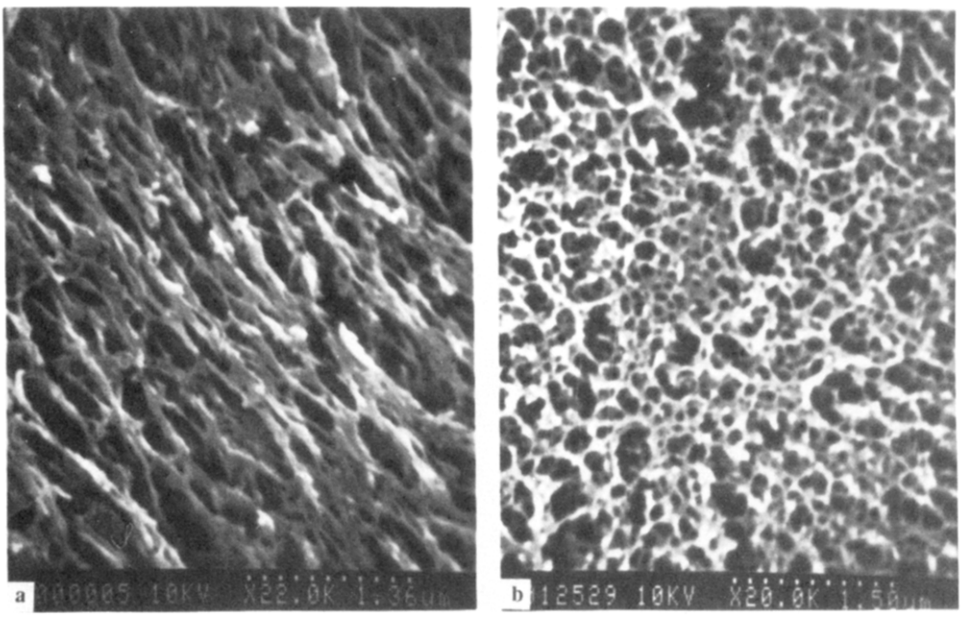

Figure 13. Scanning electron micrograph of the surface of the PMMA membrane in contact with the thermal-insulator plate. The membrane was prepared by quenching a 17.5 wt % PMMA solution (a) directly into liquid nitrogen and (b) to 34 °C and holding for 5 min.

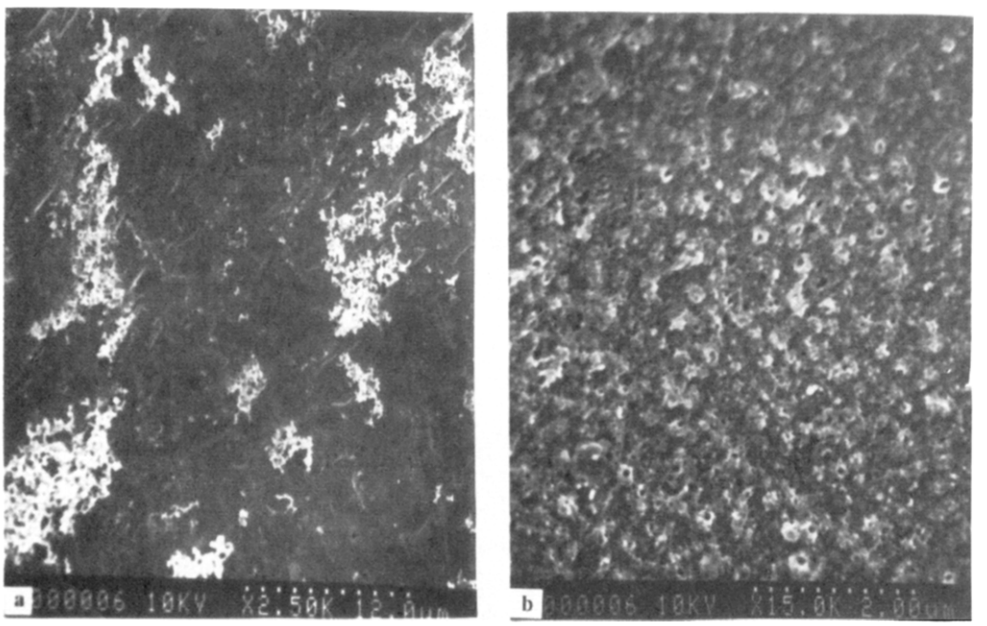

Figure 14. Scanning electron micrograph of the surface of the PMMA membrane in contact with the thermal-conductor plate. The membranes were prepared by quenching (a) a 10 wt % PMMA solution and (b) a 17.5 wt % PMMA directly into liquid nitrogen.

dense structure in comparison with the other portion of the membrane.

Summary

The cloud point and spinodal curves of a secondary standard PMMA/sulfolane system have been determined successfully by optical density methods and differential scanning calorimetry, respectively. Through the thermally induced phase separation process, asymmetric membranes can be made successfully for this PMMA/sulfolane system. In the later stages of phase separation by spinodal decomposition as well as nucleation and growth, coarsening plays a vital role in determining the final membrane microstructure. During the very early stage of phase separation by spinodal decomposition, a membrane with lacy structure results. In contrast, a structure composed of strings of small beads is a consequence of the early stages of phase separation by nucleation and growth. A lacy structure can also be obtained for nucleation and growth due to the effects of ripening or coalescence. For membranes prepared by quickly quenching polymer solutions into the demixing region, the membrane morphology observed by scanning electron microscopy can be interpreted consistently in accordance with the location of the metastable and unstable regions as determined by differential scanning calorimetry. For a very viscous system, this thermally induced phase separation method followed by freeze-drying may offer an opportunity to locate the spinodal curve. This study indicates that a detailed phase diagram is the key to a true understanding of the formation of microcellular structure. Even though our study emphasizes the formation of asymmetric membranes, the results are applicable to the formation of microcellular foams and other

Figure 15. Scanning electron micrograph of the cross-section of a PMMA membrane. The membranes were prepared by quenching a 5 wt % PMMA solution to 27 °C and holding for 5 min. The dense surface is the surface in contact with the thin aluminum sheet.

porous membranes which can be prepared by the thermally induced phase separation process.

Acknowledgment. We gratefully acknowledge the financial support of the National Science Foundation through a Presidential Young Investigator Award, the 3M Co., and Northwestern University. We also thank the Materials Research Center at Northwestern University for use of the scanning electron microscope.

References and Notes

(1) Kesting, R. E. *Synthetic Polymeric Membranes*; Wiley-Interscience: New York, 1985.
(2) *Chem. Eng. News* **1978**, *56* (Dec 11), 23–24.
(3) Castro, A. J. U.S. Patent 4 247 498, Jan 27, 1981.
(4) Coudeville, A.; Eyharts, P.; Perrine, J. D.; Rouillard, R. *J. Vac. Sci. Technol.* **1981**, *18*, 1227.
(5) Young, A. T.; Moreno, D. K.; Marsters, R. G. *J. Vac. Sci. Technol.* **1982**, *20*, 1094.
(6) Aubert, J. H.; Clough, R. L. *Polymer* **1985**, *26*, 2047.
(7) Williams, J. M.; Moore, J. E. *Polymer* **1987**, *28*, 1950.
(8) Sylwester, A. P.; Aubert, J. H.; Rand, P. B.; Arnold, C., Jr.; Clough, R. L. *Polym. Mater. Sci. Eng.* **1987**, *57*, 113.
(9) Aubert, J. H.; Sylwester, A. P.; Rand, P. B. *Polym. Prepr. (Am. Chem. Soc., Div. Polym. Chem.)* **1989**, *30*(1), 447.
(10) Jackson, C. L.; Samulski, E. T.; Shaw, M. T. *Polym. Mater. Sci. Eng.* **1987**, *57*, 107.
(11) Hikmer, R. M.; Callister, S.; Keller, A. *Polymer* **1988**, *29*, 1378.
(12) Aubert, J. H. *Macromolecules* **1988**, *21*, 3468.
(13) Stoks, W.; Berghmans, H.; Moldenaers, P.; Mewis, J. *Br. Polym. J.* **1988**, *20*, 361.
(14) Hiatt, W. C.; Vitzthum, G. H.; Wagener, K. B.; Josefiak, C. In *Materials Science of Synthetic Membranes*; Lloyd, D. R., Ed.; ACS Symp. Ser. 269; American Chemical Society: Washington, 1985; pp 229–244.
(15) Vitzthum, G. H.; Davis, M. A. U.S. Patent 4 490 431, Dec 25, 1984.
(16) Shipman, G. H. U.S. Patent 4 539 256, Sept 3, 1985.
(17) Lloyd, D. R.; Barlow, J. W.; Kinzer, K. E. In *New Membrane Materials and Processes for Separation*; Sirkar, K. K., Lloyd, D. R., Eds.; AIChE Symp. Ser. 261; American Institute of Chemical Engineers: New York, 1988; Vol. 84, pp 28–41.
(18) Caneba, G. T.; Soong, D. S. *Macromolecules* **1985**, *18*, 2538.
(19) Caneba, G. T.; Soong, D. S. *Macromolecules* **1985**, *18*, 2545.
(20) Tsai, F.-J.; Torkelson, J. M. In *Biological and Synthetic Membranes*; Butterfield, D. A., Ed.; Alan R. Liss, Inc.: New York, 1989; Progress in Clinical and Biological Research, Vol. 292, pp 119–128.
(21) Smolders, C. A.; van Aartsen, J. J.; Steenbergen, A. *Kolloid-Z. Z. Polym.* **1971**, *243*, 14.
(22) Broens, L.; Altena, F. W.; Smolders, C. A.; Koenhen, D. M. *Desalination* **1980**, *32*, 33.
(23) Arnauts, J.; Berghmans, H. *Polym. Commun.* **1987**, *28*, 66.
(24) Cahn, J. W.; Hilliard, J. E. *J. Chem. Phys.* **1958**, *28*, 258.
(25) Hilliard, J. E. In *Phase Transformations*; Aaronson, H. I., Ed.; American Society for Metals: Metal Park, OH, 1970; pp 497–560.
(26) van Emmerik, P. T.; Smolders, C. A.; Geymayer, W. *Eur. Polym. J.* **1973**, *9*, 309.
(27) Nojima, S.; Shiroshita, K.; Nose, T. *Polym. J.* **1982**, *14*, 289.
(28) Tsai, F.-J.; Torkelson, J. M. *Macromolecules* **1988**, *21*, 1026.
(29) Caneba, G. T.; Soong, D. S. *Macromolecules* **1985**, *19*, 369.
(30) Scott, R. L. *J. Chem. Phys.* **1945**, *13*, 178.
(31) Kurata, M. *Thermodynamics of Polymer Solutions*; translated by Fujita, H.; Harwood Academic Publishers: New York, 1982; Vol. 1, pp 87–91.
(32) van Emmerik, P. T.; Smolders, C. A. *Eur. Polym. J.* **1973**, *9*, 293.
(33) (a) *Catalog Handbook of Fine Chemicals*; Aldrich Chemical Co., 1988–1989; T2,220-9, p 1410. (b) *The Merck Index*, 9th ed.; 1976, p 1160.
(34) McMaster, L. P. *Adv. Chem. Ser.* **1975**, *No. 142*, 43.
(35) Coarsening may play a role in determining the microstructure of this membrane formed by slow cooling.

Registry No. PMMA, 9011-14-7.